AIP | Applied Physics Letters

In situ synchrotron X-ray diffraction study of deformation behavior and load transfer in a Ti2Ni-NiTi composite

Junsong Zhang, Yinong Liu, Yang Ren, Yong Huan, Shijie Hao, Cun Yu, Yang Shao, Yadong Ru, Daqiang Jiang, and Lishan Cui

Citation: Applied Physics Letters **105**, 041910 (2014); doi: 10.1063/1.4892352
View online: http://dx.doi.org/10.1063/1.4892352
View Table of Contents: http://scitation.aip.org/content/aip/journal/apl/105/4?ver=pdfcov
Published by the AIP Publishing

In situ synchrotron X-ray diffraction study of deformation behavior and load transfer in a Ti_2Ni-NiTi composite

Junsong Zhang,[1] Yinong Liu,[2] Yang Ren,[3] Yong Huan,[4] Shijie Hao,[1] Cun Yu,[1] Yang Shao,[1] Yadong Ru,[1] Daqiang Jiang,[1] and Lishan Cui[1,a)]
[1]*Department of Materials Science and Engineering, China University of Petroleum-Beijing, Changping, Beijing 102249, China*
[2]*School of Mechanical and Chemical Engineering, The University of Western Australia, Crawley, WA 6009, Australia*
[3]*X-ray Science Division, Argonne National Laboratory, Argonne, Illinois 60439, USA*
[4]*State Key Laboratory of Nonlinear Mechanics (LNM), Institute of Mechanics, Chinese Academy of Sciences, Beijing 100190, China*

(Received 10 June 2014; accepted 16 July 2014; published online 31 July 2014)

The deformation behavior and load transfer of a dual-phase composite composed of martensite NiTi embedded in brittle Ti_2Ni matrices were investigated by using *in situ* synchrotron x-ray diffraction during compression. The composite exhibits a stage-wise deformation feature and a double-yielding phenomenon, which were caused by the interaction between Ti_2Ni and NiTi with alternative microscopic deformation mechanism. No load transfer occurs from the soft NiTi dendrites to the hard Ti_2Ni matrices during the pseudoplastic deformation (detwinning) of NiTi, which is significantly different from that previously reported in bulk metallic glasses matrices composites.
 [http://dx.doi.org/10.1063/1.4892352]

Soft/hard dual-phase composites are capable of exhibiting coupled high strength and large ductility simultaneously.[1–4] Their enhanced mechanical properties generally stem from the interaction between the soft component and the hard component during deformation.[1–4] Traditional metal matrix composites (MMCs) are one of the most common soft/hard dual-phase composite, which consist of a hard yet brittle reinforcement dispersed in a soft and ductile metallic matrix.[5–12] In the past two decades, with the goal of improving the plasticity of high-strength but brittle materials (such as nanostructured materials and bulk metallic glasses), ductile dendrites with lower yield strength were introduced to embed in these high-strength but brittle matrices.[1,2,13–20] During loading, the dendrite phase first exceeds its yield strength and undergoes plastic deformation, whereas the high-strength matrix remains elastic and followed by brittle fracture.[18,20] These kinds of dual-phase composites exhibit significant differences in their mechanical behavior as compared to traditional MMCs.[7,8,17,19]

In the previously reported nanostructured-matrix composites or bulk metallic glasses matrices composites, the ductile dendrites flow occurs primarily by dislocation slip.[1,2,17,20] These composites undergo first elastic deformation followed by plastic deformation and often exhibit one-time yielding.[1,2,17,20] However, little is known about the mechanical behavior of these kinds of dual-phase composites in which the ductile dendrites exhibiting alternative deformation mechanisms (e.g., stress-induced martensitic transformation or martensite variant detwinning). In this work, the microscopic deformation mechanism and load transfer in a dual-phase composite composed of martensite NiTi embedded in brittle Ti_2Ni matrices, where the ductile NiTi component deforms by martensite variant detwinning (pseudoplasticity), were studied by using *in situ* synchrotron-based high-energy X-ray diffraction (HEXRD) during compressive test.

An alloy ingot of ~100 g with a nominal composition of $Ti_{54}Ni_{46}$ (at. %) was prepared from commercial Ti and Ni elements of 99.99 wt. % purity by arc melting under argon atmosphere in a water-cooled copper hearth. The microstructure observation of the composite was characterized using a FEI-200F scanning electron microscope (SEM) equipped with an energy-dispersive x-ray spectrometer (EDX) operated at accelerating voltage of 20 kV. In order to evaluate the mechanical properties under compression, cylindrical samples of 4 mm in diameter and 8 mm in length were prepared and tested by using a servo-hydraulic materials testing system (MTS 810) at a strain rate of 5×10^{-4} s^{-1} at room temperature. An *in situ* synchrotron-based HEXRD measurement during compression test was performed on the 11-ID-C beam line of the Advanced Photon Source, Argonne National Laboratory, USA. A monochromatic high-energy X-rays with a energy of 115 keV, beam size of 0.6×0.6 mm^2, and wavelength of 0.10798 Å were used to obtain two-dimensional (2-D) diffraction patterns in transmission configuration. One-dimensional (1-D) HEXRD diffraction patterns under various applied strains were obtained by integrating along the specified azimuthal angle over a range of ±10 in the 2-D diffraction patterns.

Fig. 1 shows the as-cast microstructure of Ti_2Ni-NiTi composite. The main diffraction peaks in HEXRD pattern (as shown in Fig. 1(a)) of the composite can be identified as a mixture of monoclinic $P2_1/m$ NiTi ($B19'$) and face-centered cubic (fcc) $Fd3m$ Ti_2Ni intermetallic compound. Fig. 1(b) reveals the micro-morphology of the composite characterized by SEM. The NiTi (gray phase) dendrites, with size of up to several tens of micrometers, are homogeneously dispersed in the Ti_2Ni (dark phase) matrix. Quantitative image analysis of SEM micrograph displays that the phase volume fraction of the NiTi dendrites is about 75%.

a)Author to whom correspondence should be addressed. Electronic mail: lscui@cup.edu.cn

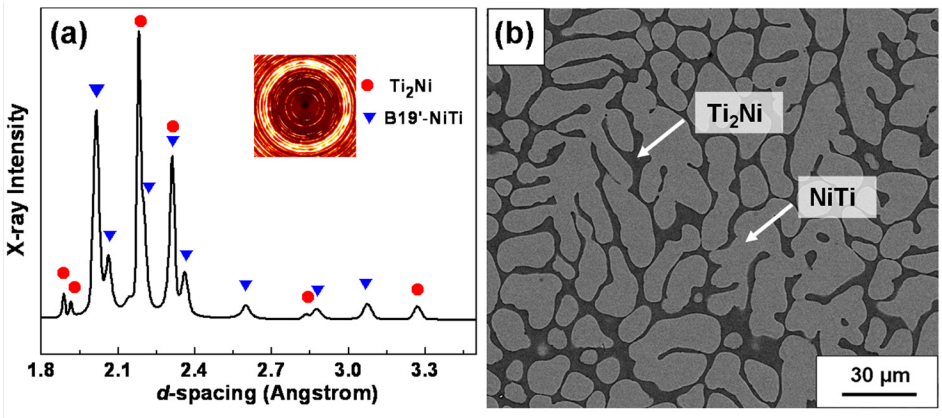

FIG. 1. 1-D HEXRD pattern (a) and SEM backscattered electron micrograph (b) of the Ti_2Ni-NiTi composite.

Fig. 2 presents the engineering compressive stress-strain curve of the Ti_2Ni-NiTi composite at room temperature. The inset in Fig. 2 is the corresponding true stress-strain curve. The composite exhibits about 24% plastic strain prior to fracture, and the ultimate compressive strength reaches 2350 MPa. Obviously, high strain hardening is evident (shown in the inset in Fig. 2). It is worthy to note that the composite shows a double yielding phenomenon. The first yielding occurs at about 300 MPa, while the second yielding happens at approximate 1300 MPa. The engineering compressive stress-strain curve of the composite can be divided into three stages: <4% (I), 4%–10% (II), >10% (III) of applied strain, by turnings from post yielding stages to strain hardening stages. This special mechanical behavior may be related to the interaction between the brittle Ti_2Ni matrices and the ductile NiTi dendrites deforming by specific mechanisms.

To understand the unique mechanical behavior of this composite, *in situ* synchrotron HEXRD measurements were carried out during compressive test. Fig. 3(a) shows one-dimensional diffraction spectrum recorded in the longitudinal direction of the cylindrical sample at different applied strains from 0% to 18%. Upon loading, the B19′-NiTi and Ti_2Ni diffraction peaks are initially found shifting to lower *d*-spacing values, which demonstrate the elastic deformation of both components in the composite under compression.

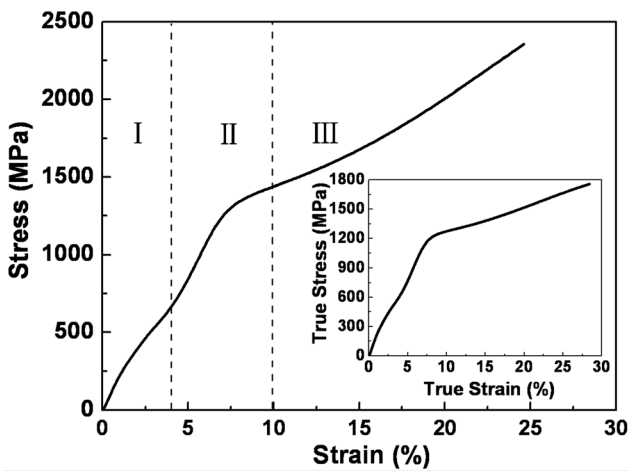

FIG. 2. Room temperature compressive engineering stress-strain curve of the Ti_2Ni-NiTi composite. The inset is its true stress-strain curve.

With increasing of the applied strain, the *d*-spacing values of both components remain almost constant or decrease very slowly, indicating the plastic deformations. Meanwhile, the diffraction peaks broadening is found and their peak intensity increases with increasing applied strain, which implies the increased inhomogeneity in strain fields which is related to increased defects density.

From Fig. 3(a), it also can be seen that the intensity of B19′-NiTi (100) diffraction peak increases whilst the intensity of B19′-NiTi ($\bar{1}11$) diffraction peak decreases, which indicates that the martensite variant reorients via detwinning (pseudoelasticity). More evidence of variants reorientation process is shown in Fig. 3(b). Combining Figs. 3(a) and 3(b), we can see that martensitic variants with (100) and (111) planes perpendicular to the loading direction grow at the expense of variants with ($\bar{1}11$), (020), and (001) planes perpendicular to the loading direction. That is, during compression, variants with (100) and (111) planes tend to orients toward the loading direction, while variants with ($\bar{1}11$), (020), and (001) planes are aligned to the transverse direction. This result is also consistent with crystallographic analysis of the B19′ martensite.[21]

Fig. 3(c) reveals the lattice strain evolution of B19′-NiTi (100) and Ti_2Ni (511) along the loading direction as a function of the applied strain. The lattice strain is calculated from the diffraction peak positions using $\varepsilon_{hkl} = |d_{hkl} - d_{hkl}^0| / d_{hkl}^0$, where d_{hkl}^0 is the peak position at zero applied stress. Upon loading, the lattice strains for both B19′-NiTi and Ti_2Ni increase rapidly with increasing the applied strain in the initial deformation stage (<1% applied strain), indicating the elastic deformation of these two phases. From 1% to 4% of the applied strain, the lattice strain of Ti_2Ni continues to increase indicating further elastic deformation, whereas the lattice strain of B19′-NiTi remains almost constant which indicates that the deformation is caused by martensite reorientations. This implies that the increasing in external applied stress is primarily borne by the Ti_2Ni matrix. Meanwhile, the first yield point on stress-strain curve is attributed to the onset of martensite variant reorientation deformation of NiTi dendrites.

Beyond the applied strain of 4%, the lattice strain of NiTi begins to increase rapidly again until the applied strain of 10%, which is caused by the completion of martensite variant reorientation and the commencement of the elasto-plastic deformation of oriented martensite. At above the

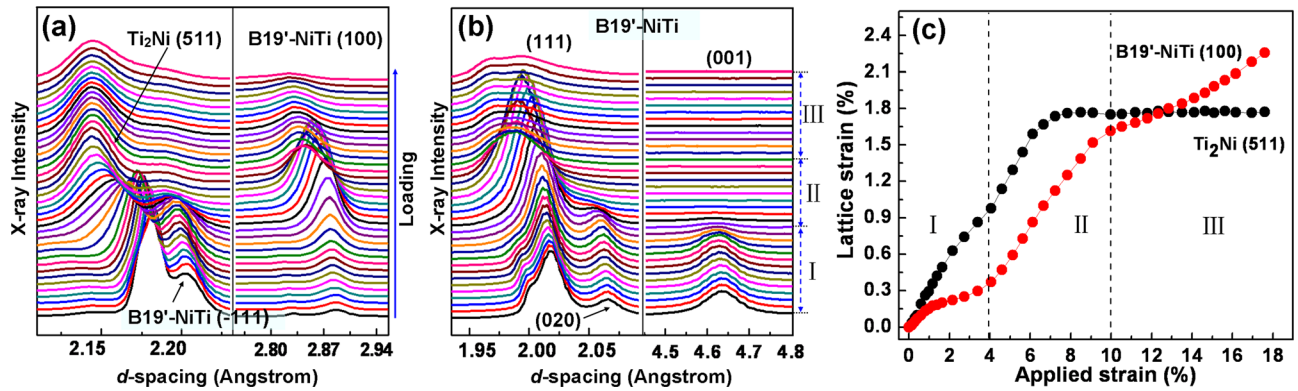

FIG. 3. (a) and (b) One-dimensional diffraction pattern recorded in the longitudinal direction at different levels of applied strain. (c) Evolution of the lattice strain with respect to the applied strain for the Ti_2Ni (511) plane and B19′-NiTi (100) plane perpendicular to the loading direction in the composite.

applied strain of 10%, massive plastic deformation and strain-hardening of the reoriented martensite occur, resulting in the lattice strain of NiTi increasing at a lower rate. In contrast, the lattice strain of Ti_2Ni still increases at a high rate followed by an apparent "yielding" at about 7% applied strain and then remains constant. Therefore, the second yield point of stress-strain curve is resulted from the yielding of the Ti_2Ni matrix. In deformation stage III (>10% applied strain), since the lattice strain of Ti_2Ni remains constant, the further moderate increase in external stress (see Fig. 2 and the inset in Fig. 2) is clearly caused by the strain-hardening of the NiTi reoriented martensite.

Fig. 4 shows the applied stress as a function of lattice strain for B19′-NiTi (100) and Ti_2Ni (511) planes perpendicular to the loading direction. The three deformation stages in Fig. 4 are consistent with the deformation stages divided in stress-strain curve shown in Fig. 2. The lattice strain of NiTi increases linearly in the initial stage due to the elastic deformation ("O-A"), thereupon turns upward caused by the martensite variant reorientation ("A-B"), followed by a rapid increasing rate owing to the elasto-plastic deformation of oriented martensite ("B-C-D"), and then increasing at a relatively slow rate resulted from the plastic deformation (after point D). At an applied stress of about 1250 MPa (point C), the lattice strain slope for NiTi has changed and becomes small, which implies an increase in the fraction of the load being transferred to the NiTi. This load transfer is caused by the yielding of the Ti_2Ni matrix, which is similar to the bulk metallic glasses composite where the brittle glasses matrices invariably transfer the load to the soft dendrites as its yielding.[17,18,20] Interestingly, although the deformation mechanism of NiTi undergoes stage-wise change ("O-A-B-C"), the slope of Ti_2Ni lattice strain almost constant until it yielding (after point C). It means that no load transfer occurs from the NiTi to the Ti_2Ni matrix during the pseudoplastic deformation of NiTi via martensite variant detwinning. This is entirely different from the previously reported dual-phase composites where, due to the plastic misfit induced by dislocation slip of the soft phase, the load is always transferred from the soft component to the hard component.[7,9,17,20] We conjecture that the plastic misfit caused by the martensite variant reorientation (detwinning) is lower than the plastic mismatch induced by dislocation slip, and thus results in very little or no load transfer between NiTi and Ti_2Ni during the stage of martensite variant reorientation (detwinning).

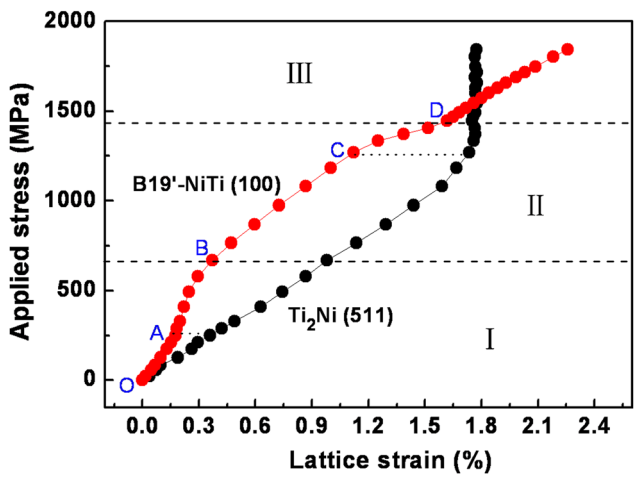

FIG. 4. Plot of applied stress versus lattice strain of B19′-NiTi (100) plane and Ti_2Ni (511) plane perpendicular to the loading direction.

To summarize, a unique dual-phase composite consisting of the NiTi shape memory alloy embedded in the brittle Ti_2Ni matrix was fabricated. The composite displays a three-stage deformation behavior and two-yield point phenomenon. The first stage is ascribed to the initial elasticity and the reorientation deformation of the martensite NiTi and the elastic deformation of Ti_2Ni. The onset of martensite variant reorientation leads to the first yield point of the composite. The second stage is mainly controlled by the deformation of Ti_2Ni, while the NiTi oriented martensite remains elasto-plastic deformation. The yielding of Ti_2Ni matrix results in the second yield point of the composite. The strain-hardening of the composite in the third stage is related to the strain-hardening of the NiTi reoriented martensite. There is no load transfer from NiTi to Ti_2Ni matrix when the NiTi experiences stress-induced martensite variant reorientation. This study provides in-depth understanding of the deformation behavior and load transfer of the composite consisted of hard yet brittle materials as the matrix and shape memory alloy as the reinforcement.

This work was supported by the key program project of National Natural Science Foundation of China (NSFC) (Grant No. 51231008), the National 973 programs of China

(Grant No. 2012CB619403), the Australian Research Council (Grant No. DP140103805), and the Key Project of Chinese Ministry of Education (Grant No. 313055). The use of the Advanced Photon Source was supported by the US Department of Energy, Office of Science, and Office of Basic Energy Science, Office of Basic Energy Sciences, under Contract No. DE-AC02-06CH11357.

[1]G. He, J. Eckert, W. Löser, and L. Schultz, Nat. Mater. **2**, 33 (2003).
[2]D. C. Hofmann, J. Y. Suh, A. Wiest, G. Duan, M. L. Lind, M. D. Demetriou, and W. L. Johnson, Nature **451**, 1085 (2008).
[3]S. H. Xia and J. T. Wang, Int. J. Plast. **26**, 1442 (2010).
[4]J. W. Qiao, T. Zhang, F. Q. Yang, P. K. Liaw, S. Pauly, and B. S. Xu, Sci. Rep. **3**, 2816 (2013).
[5]L. Wang, M. Li, and J. Almer, Acta Mater. **62**, 239 (2014).
[6]V. Y. Mehr, M. R. Toroghinejad, and A. Rezaeian, Mater. Sci. Eng., A **601**, 40 (2014).
[7]D. H. Bacon, L. Edwards, J. E. Moffatt, and M. E. Fitzpatrick, Acta Mater. **59**, 3373 (2011).
[8]N. Jia, Z. H. Cong, X. Sun, S. Cheng, Z. H. Nie, Y. Ren, P. K. Liaw, and Y. D. Wang, Acta Mater. **57**, 3965 (2009).
[9]M. L. Young, J. DeFouw, J. D. Almer, and D. C. Dunand, Acta Mater. **55**, 3467 (2007).
[10]S. J. Hao, D. Q. Jiang, L. S. Cui, Y. D. Wang, X. B. Shi, Z. H. Nie, D. E. Brown, and Y. Ren, Appl. Phys. Lett. **99**, 084103 (2011).
[11]L. Thilly, S. V. Petegem, P. O. Renault, F. Lecouturier, V. Vidal, B. Schmitt, and H. V. Swygenhoven, Acta Mater. **57**, 3157 (2009).
[12]L. Thilly, P. O. Renault, V. Vidal, F. Lecouturier, S. V. Petegem, U. Stuhr, and H. V. Swygenhoven, Appl. Phys. Lett. **88**, 191906 (2006).
[13]J. Mu, Z. W. Zhu, R. Su, Y. D. Wang, H. F. Zhang, and Y. Ren, Acta Mater. **61**, 5008 (2013).
[14]S. Pauly, G. Liu, G. Wang, J. Das, K. B. Kim, U. Kühn, D. H. Kim, and J. Eckert, Appl. Phys. Lett. **95**, 101906 (2009).
[15]M. M. Trexler and N. N. Thadhani, Prog. Mater. Sci. **55**, 759 (2010).
[16]C. P. Kim, Y. S. Oh, S. Lee, and N. J. Kim, Scr. Mater. **65**, 304 (2011).
[17]R. T. Ott, F. Sansoz, J. F. Molinari, J. Almer, K. T. Ramesh, and T. C. Hufnagel, Acta Mater. **53**, 1883 (2005).
[18]D. K. Balch, E. Üstündag, and D. C. Dunand, J. Non-Cryst. Solids **317**, 176 (2003).
[19]D. K. Balch, E. Üstündag, and D. C. Dunand, Metall. Mater. Trans. A **34**, 1787 (2003).
[20]Z. Zhu, H. Zhang, Z. Hu, W. Zhang, and A. Inoue, Scr. Mater. **62**, 278 (2010).
[21]D. C. Dunand, D. Mari, M. A. M. Bourke, and J. A. Roberts, Metall. Mater. Trans. A **27**, 2820 (1996).